Elastic properties of DNA linked flexible magnetic filaments

2008 J. Phys.: Condens. Matter 20 204107

(http://iopscience.iop.org/0953-8984/20/20/204107)

IOP PUBLISHING JOURNAL OF PHYSICS: CONDENSED MATTER
J. Phys.: Condens. Matter **20** (2008) 204107 (5pp) doi:10.1088/0953-8984/20/20/204107

Elastic properties of DNA linked flexible magnetic filaments

K Ērglis[1], D Zhulenkovs[2], A Sharipo[2] and A Cēbers[1]

[1] Department of Theoretical Physics, University of Latvia, Zellu 8, Riga, LV-1002, Latvia
[2] Latvian Biomedical Research and Study Center, Ratsupites 1, Riga, LV-1067, Latvia

E-mail: aceb@tesla.sal.lv

Received 1 April 2008
Published 1 May 2008
Online at stacks.iop.org/JPhysCM/20/204107

Abstract
Elastic properties of magnetic filaments linked by DNA in solutions of univalent and bivalent salts with different pH values are investigated through their deformation in an external field. A strong dependence of the bending modulus in bivalent salt solution on the pH is shown. Experimental results are interpreted on the basis of the magnetic elastica.

1. Introduction

Flexible magnetic filaments recently created by linking superparamagnetic particles with polymeric molecules [1, 2] possess different interesting properties. Among some of their applications are those in micromechanical sensors [1, 3] and as mixers for microfluidics [4, 5]; and they can be used for the creation of microengines which are driven by an external ac magnetic field [6, 7]. A unifying description of the behavior of these filaments is suggested in [8] where the nonlinear PDE are derived by extension of the classical model of the Kirchhoff rod taking into account its magnetic properties. This model predicts buckling instability of a filament oriented perpendicularly to the external field. Due to this instability characteristic hairpin structures arise, which can be used to determine mechanical properties of the linking polymer [9]. These hairpin structures belong to the family of elastica known from the study of elastic rods under the action of compressional stress [10].

Since DNA linking the superparamagnetic particles is a polyelectrolyte bearing one elementary charge per 0.17 nm, according to the existing models of semiflexible polyelectrolyte chains [11, 12] the stiffening of the filaments at low salt concentration may be expected. Here, measurements of the bending elasticity of the filaments in a broad range of monovalent and bivalent salt solutions at several pH values are carried out and the results are interpreted on the basis of the magnetic elastica solutions.

2. Models

The energy of a magnetic filament includes its bending energy characterized by the bending modulus C and the energy of interaction with the external field, which depends on the orientation of the local element of the filament

$$E = \frac{1}{2}C\int\left(\frac{\mathrm{d}\vartheta}{\mathrm{d}l}\right)^2 \mathrm{d}l - \frac{a^2(\mu-1)^2}{8(\mu+1)}H_0^2\int\cos^2\vartheta\,\mathrm{d}l. \quad (1)$$

Here ϑ is the angle between the tangent to the filament $\vec{t} = (\cos\vartheta, \sin\vartheta)$ and the direction of the external field H_0, a is the radius of the filament, μ is its magnetic permeability. Minimizing the energy (1) with respect to the variation of the tangent of angle ϑ the Euler–Lagrange equation reads

$$-C\frac{\mathrm{d}^2\vartheta}{\mathrm{d}l^2} + \frac{a^2(\mu-1)^2H_0^2}{8(\mu+1)}\sin 2\vartheta = 0. \quad (2)$$

If the length of the filament is $2L$, then in dimensionless form the problem is as follows ($Cm = a^2(\mu+1)^2H_0^2L^2/8(\mu+1)C$ is the magnetoelastic number [8]):

$$-\frac{\mathrm{d}^2\vartheta}{\mathrm{d}l^2} + Cm\sin 2\vartheta = 0 \quad (3)$$

with the boundary conditions at unclamped ends $\mathrm{d}\vartheta/\mathrm{d}l(\pm1) = 0$. The solution of equation (3) in terms of the elliptic functions reads

$$\cos\vartheta = k\,\mathrm{sn}(\sqrt{2Cm}l, k). \quad (4)$$

The modulus of elliptic function k is determined by the elliptic integral of the first kind, $K(k)$:

$$K(k) = \sqrt{2Cm}. \quad (5)$$

Since $K \geqslant \pi/2$ at $Cm_c = \pi^2/8$, the nontrivial elastica bifurcates [3].

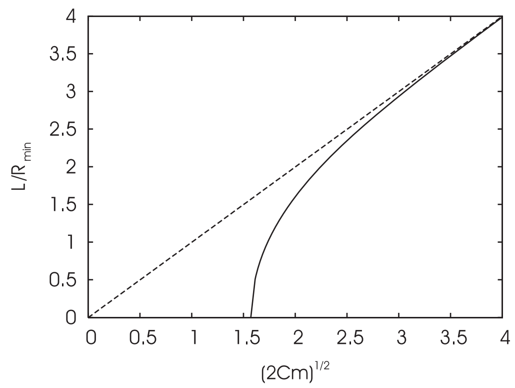

Figure 1. Maximal curvature depending on the magnetoelastic number. The asymptotic relation $L/R_{\min} = \sqrt{2\,Cm}$ is shown by a dashed line.

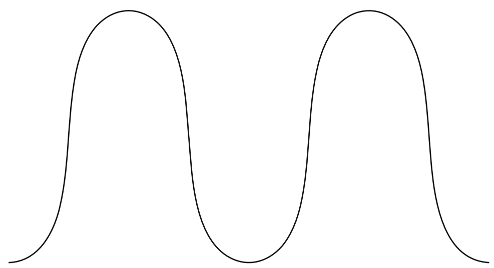

Figure 2. Elastica (4) at $Cm = 8$.

For the maximal curvature of the hairpin at its tip $l = 0$ we have

$$-\frac{\mathrm{d}\vartheta}{\mathrm{d}l} = \sqrt{2Cm}k. \tag{6}$$

For a long filament, when Cm is large we can use the asymptotics of elliptic integral $K(k) = \ln(4/\sqrt{(1-k^2)})$. In this case for the maximal curvature of the filament we have

$$\frac{L}{R_{\min}} = \sqrt{2Cm}\left(1 - 8\,\mathrm{e}^{-2\sqrt{2Cm}}\right). \tag{7}$$

We see that with a very good accuracy, in the limit of large Cm the maximal curvature $1/R_{\min}$ is linearly proportional to the magnetic field strength. This was used previously to determine the bending modulus of the magnetic filaments linked by PAA [1].

Relations (5) and (6) give the implicit dependence of the maximal curvature on the magnetoelastic number. This is shown in figure 1. We see that for the magnetoelastic number $Cm > 8$, the asymptotic relation $L/R_{\min} = \sqrt{2Cm}$ is valid with a good accuracy. The shape of the magnetic elastica at $Cm = 8$ for two periods is shown in figure 2. Important for experiment is the question of the stability of the elastica. It is interesting that using the properties of elliptic functions it is possible to give an exact answer to this question.

Introducing the scalings as described above, the energy functional can be rewritten as follows:

$$E = \frac{1}{2}\frac{C}{L}\int\left[\left(\frac{\mathrm{d}\vartheta}{\mathrm{d}l}\right)^2 - 2\,Cm\cos^2\vartheta\right]\mathrm{d}l. \tag{8}$$

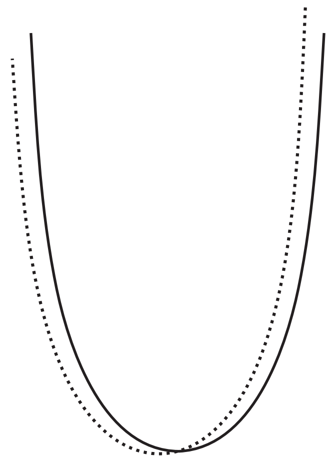

Figure 3. Unstable perturbation mode for the elastica proportional to $\mathrm{d}n(l,k)$ (dashed line), elastica (4) (solid line). Development of perturbation leads to the increase of the difference of the lengths of the hairpin legs. $Cm = 8$.

Its second variation reads (ϑ_0 for the elastica (4))

$$\delta^2 E = \frac{C}{L}\int\left[\frac{\mathrm{d}\delta\vartheta}{\mathrm{d}l}\frac{\mathrm{d}\delta\vartheta}{\mathrm{d}l} + 2\,Cm\cos 2\vartheta_0(\delta\vartheta)^2\right]\mathrm{d}l. \tag{9}$$

The Euler–Lagrange equation for functional $\delta^2 E/\int(\delta\vartheta)^2\,\mathrm{d}l$ gives an eigenvalue problem for the linear operator $\hat{L} = -\frac{\mathrm{d}^2}{\mathrm{d}l^2} + 2\,Cm\cos 2\vartheta_0$:

$$\hat{L}\delta\vartheta = \lambda\delta\vartheta. \tag{10}$$

Existence of negative eigenvalues λ corresponds to the instability of the magnetic elastica (4). Introducing $\tilde{l} = \sqrt{2\,Cm}\,l$, equation (10) reads (tildes are omitted)

$$\frac{\mathrm{d}^2}{\mathrm{d}l^2}\delta\vartheta - (2k^2\,\mathrm{sn}^2(l,k) - 1)\delta\vartheta = -\frac{\lambda}{2\,Cm}\delta\vartheta. \tag{11}$$

Since the elliptic function $\mathrm{d}n(l,k)$ satisfies the equation

$$\frac{\mathrm{d}^2\mathrm{d}n(l,k)}{\mathrm{d}l^2} - (2k^2\,\mathrm{sn}^2(l,k) - k^2)\,\mathrm{d}n(l,k) = 0. \tag{12}$$

and the boundary conditions $\mathrm{d}\delta/\vartheta\mathrm{d}l(\pm 1) = 0$, $\lambda = -2\,Cm(1-k^2)$ is the eigenvalue.

For large Cm values $\lambda = -32\;Cm\,\mathrm{e}^{-2\sqrt{2\,Cm}}$ and the eigenvalue is exponentially small. Thus hairpins should be observed as long living transient states. A similar result is obtained by numerical analysis in [13].

Shapes of perturbed and unperturbed hairpins are shown in figure 3 for $Cm = 8$. Development of the perturbation mode shown in figure 3 has been observed in numerical simulations [8].

An important issue is the origin of the stiffness of magnetic filaments. According to the technology of their production, described in the next section, the linking of the superparamagnetic particles occurs by adsorption of biotinylated fragments of DNA with definite length on the superparamagnetic particles functionalized by streptavidin.

To estimate the number of DNA molecules attached to the particles with a radius a we assume that the maximal distance

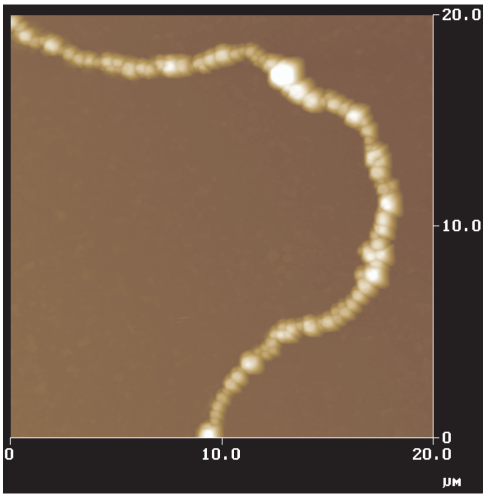

Figure 4. AFM scan of a magnetic filament. Courtesy of J Winer, Qi Wen and P A Janmey.

(This figure is in colour only in the electronic version)

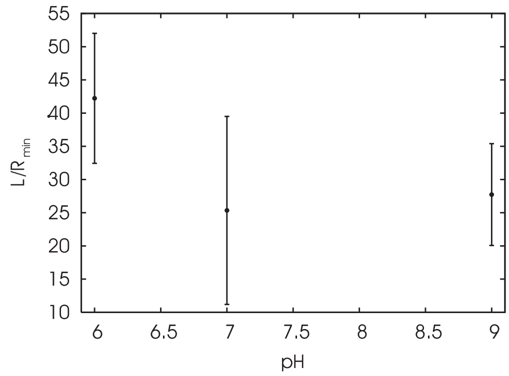

Figure 5. Maximal curvature depending on the pH. $H_0 = 40.8$ Oe.

between the adsorbing sites on the particles connected with a DNA molecule is equal to the persistence length of dsDNA l_p or 50 nm in salt solution with a high ionic force. Then for the radius of the bundle R_b linking the particles ($l_p \gg h$) (h is the distance between the particles) we have the estimate $R_b = \sqrt{a l_p}$. The curvature of the link between particles on the deformation of the filament can be estimated according to the similarity argument $1/R_l = \frac{2a}{h} \cdot \frac{1}{R}$ [1], where R is the curvature of the filament. This for the effective bending modulus of the filament gives $C = \frac{2a}{h} C_b$, where C_b is the bending modulus of the bundle. We estimate it by multiplying the bending modulus of the single DNA molecule $k_B T l_p$ by the number of molecules presumably participating in the link, $\pi R_b^2/l_a^2$, where $l_a = 2.2$ nm is the distance between the streptavidin sites, based on the data from the supplier. According to the model of semiflexible polyelectrolyte chains [11, 12], then

$$C = k_B T \frac{2\pi a^2}{h l_a^2} \left(l_p^0 + \frac{l_B l_D^2}{4b^2} \right)^2 . \qquad (13)$$

Here $l_p^0 = 50$ nm is the DNA persistence length at high ionic strength, $l_B = e^2/\varepsilon k_B T$ is the Bjerrum length, l_D is the Debye length for univalent salt calculated according to the relation $l_D = 0.3/\sqrt{c}$, and $b = 0.17$ nm is the distance between elementary charges on the DNA backbone.

3. Materials and methods

Superparamagnetic particles functionalized by streptavidin (Ademtech) have the size 0.5 μm and 10^3 pmol mg^{-1} for the biotin active sites. Biotinylated 456 bp long DNA fragments were synthesized by PCR from the plasmid template pQE–srtA (ASLA Biotech) containing the srtA gene. 5′-biotinylated primers 5′-Bio-tactatgcaagctaaacctcaattccg-3′ (direct) and 5′-Bio-tacacgagttgacttctgtagctacaagat-3′ (reverse) (Metabion) and Taq polymerase (Fermentas) from the thermophilic bacterium *T. aquaticum* were applied in 30 cycles of PCR with the temperature regime 94 °C, 57 °C and 72 °C and respective times 20 s, 20 s, 30 s resulting in strongly homogeneous 456 bp long double-stranded 5′-biotinylated DNA fragments.

Filaments were obtained in buffer solutions (PBS, TE) at the superparamagnetic particle concentration 0.36 mg μl^{-1} with excess of DNA at concentration 45 μg μl^{-1} applying the external magnetic field 500 Oe. The number of DNA molecules participating in the link between the particles was estimated as 1.6×10^4.

The AFM scan of the magnetic filaments produced as described is shown in figure 4. It gives direct evidence for the formation of linked linear chains, one particle radius thick. The bending modulus, as illustrated by the dependence of the maximal curvature on the pH values, shown in figure 5, increases proportionally to the DNA deprotonation.

Samples of the magnetic filaments for the study of their deformation under the action of a constant field were placed between two glass slides separated by 0.028 mm double-sided sticky tape with an aperture cut in the center. The constant magnetic field was created by four water-cooled coils giving a field 0–70 Oe. The deformation of the filaments was captured by a Zeiss Universal microscope and a JAI CV-S3200 video camera. The characteristics of the filaments from the registered images were obtained using the ImageJ code. The set of coordinates obtained was interpolated using cubic splines and the curvature was determined by differentiation.

4. Experimental results

Magnetic filaments at different concentrations of the NaCl salt, if not mentioned otherwise, were obtained by adding to the sample the necessary amount of 5 M NaCl solution. To obtain hairpins, the field 70.7 Oe was abruptly applied to the filaments previously oriented in the perpendicular direction. Further, the field was reduced to 40 Oe. Shapes for two filaments of different lengths are shown in figure 6.

The dependences of the maximal curvature determined as described above on the magnetic field strength for the two filaments shown in figure 6 are shown in figure 7.

Experimental results (not shown here) for the maximal curvature usually were above the theoretical line $\sqrt{2\,Cm}$. One possibility for explaining this behavior is to assume that

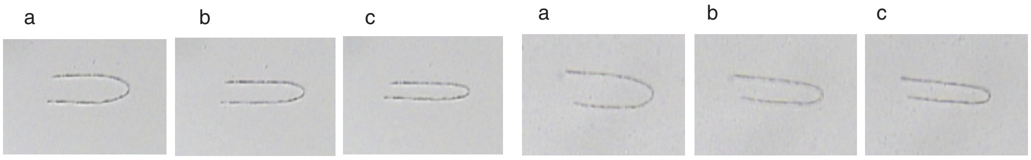

Figure 6. Buckling instability of 85 μm (left) and 90 μm (right) long filaments produced by adding to 30 μl PBS, 10 μl DNS with the concentration 180 μg ml^{-1} and 1 μl superparamagnetic particle solution with the concentration 10 mg ml^{-1} in magnetic field of 39.6 Oe (a), 56.6 Oe (b), 70.7 Oe (c). For the filament on the right, 0.15 M NaCl solution was added.

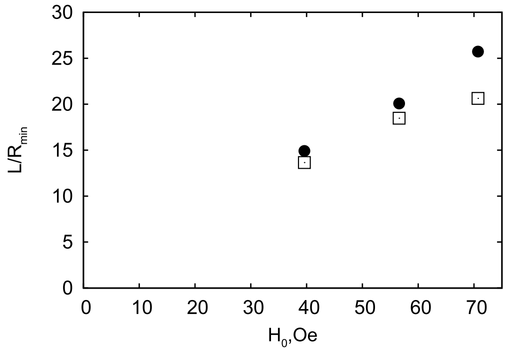

Figure 7. Maximal curvature depending on the field strength. Solid circles for the right filament in figure 6, empty squares for the left filament in figure 6.

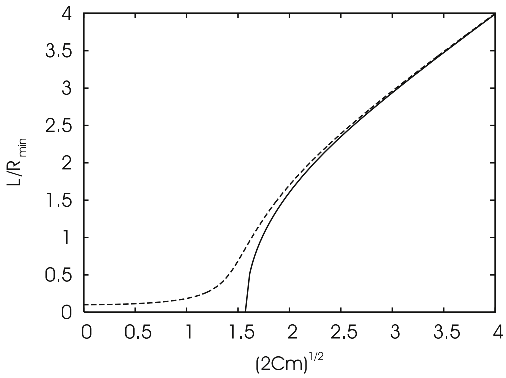

Figure 8. Maximal curvature of the filament with spontaneous curvature (dashed line). Imperfect bifurcation at the buckling can be seen.

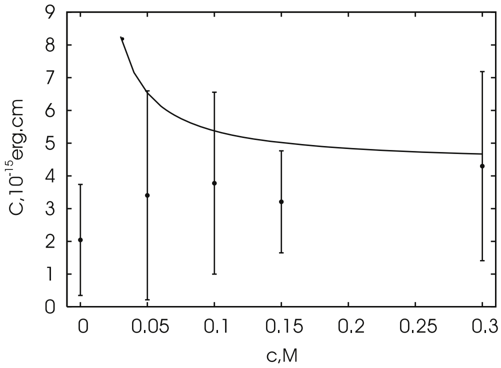

Figure 9. Bending modulus depending on the concentration of NaCl salt in TE (10 mM Tris, 1 mM EDTA, pH = 8.0).

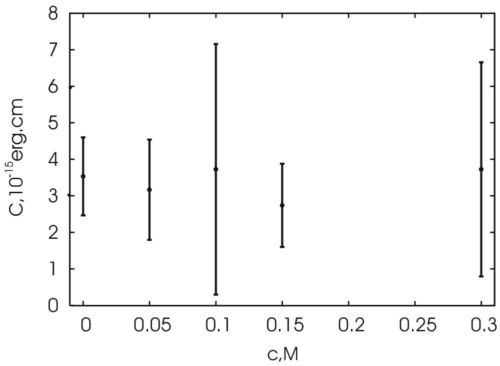

Figure 10. Bending modulus depending on the concentration of $MgCl_2$ salt in PBS (10 mM Na, K phosphate, 150 mM NaCl, pH = 7.3).

magnetic filaments possess spontaneous curvature, perhaps induced by the displacement and reconnection of DNA bundles during the deformation of the filament in the field. In this case the energy of the filament reads

$$E = \frac{1}{2} C \int \left(\frac{\mathrm{d}\vartheta}{\mathrm{d}l} + C_0 \right)^2 \mathrm{d}l - \frac{a^2(\mu - 1)^2}{8(\mu + 1)} H_0^2 \int \cos^2 \vartheta \, \mathrm{d}l. \tag{14}$$

Here C_0 is spontaneous curvature of the filament. The Euler–Lagrange equation (3) is solved with the boundary condition at the unclamped ends $-\mathrm{d}\vartheta/\mathrm{d}l(\pm 1) = LC_0$:

$$LC_0 \sqrt{1 - k^2 \,\mathrm{sn}^2(\sqrt{2\,Cm}, k)} = \sqrt{2\,Cm} k \,\mathrm{cn}\left(\sqrt{2\,Cm}, k\right) \mathrm{d}n \times \left(\sqrt{2\,Cm}, k\right). \tag{15}$$

Calculated according to the solution of equation (15), the dependence of the maximal curvature on the magnetoelastic number is shown in figure 8 at $LC_0 = 0.1$. As expected the spontaneous curvature leads to imperfect bifurcation to the hairpin solution; nevertheless this does not explain the vertical shift of the experimental values of the curvature.

For each salt concentration measurements were made on five different filaments according to the procedure shown in figures 6 and 7, allowing us to estimate the dispersion of the results, which turns out to be quite large.

A summary of the results for NaCl salt in TE is given in figure 9. The theoretical curve is drawn according to relation (13) assuming that the persistence length l_p^0 at high salt concentration 50 nm and taking $h = 30$ nm and $l_a = 5.5$ nm to match experimental data at high salt concentration. We see

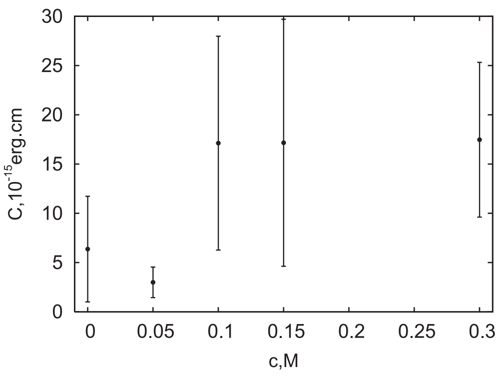

Figure 11. Bending modulus depending on the concentration of $MgCl_2$ salt in TE (pH = 7.5). The value of the bending modulus is larger than for PBS by an order of magnitude.

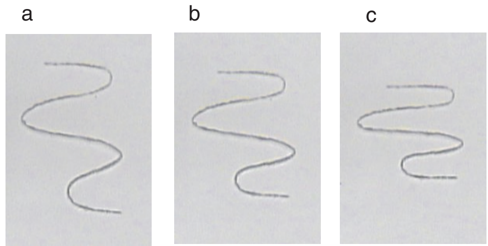

Figure 12. Buckling instability of 205 μm long filament produced by adding to 30 μl PBS 1.37 M NaCl, 10 μl DNS with concentration 180 μg ml^{-1} and 1.4 μl superparamagnetic particle solution with concentration 10 mg ml^{-1} in magnetic fields of 39.6 Oe (a), 56.6 Oe (b), 70.7 Oe (c).

that the theoretical dependence is outside the limits of the error bars. Similar results are obtained for NaCl salt in PBS. Since the distance between the DNA binding sites is close to the diameter of the dsDNA molecule, a more precise model should be developed considering the bundle of DNA.

Strong dependence of the bending modulus on the pH value (figures 10 and 11) is obtained for solutions of divalent salt $MgCl_2$ in two buffer solutions, PBS and TE.

In some cases much longer (as shown in figure 6) filaments were obtained, as illustrated in figure 12, and the formation of several hairpins was observed. This gives evidence that the most fast growing deformation mode of the filament has wavelength less than the length of the filament. Development of such a mode is expected since the protocol of the measurements carried out in the present investigation consists in abrupt application of the maximal field to induce the bending instability of the filament with further slowing of its diminishing. At slow increase of the field, filaments turn as whole to the direction along the magnetic field lines.

5. Conclusions

Deformation of flexible magnetic filaments in an external field is studied. Magnetic elastica show good agreement with the experimental data. The results obtained for the range of concentrations explored show weak dependence of the bending modulus on the concentration of salt and strong dependence in the case of bivalent salt and on the pH.

Acknowledgments

This work was financially supported by a grant from the University of Latvia 2006/1-229701, Fogarty grant R03 TW-006954-01 and ESF. The authors are grateful to their colleagues from the University of Pennsylvania P A Janmey, J Winer and Qi Wen for ongoing collaboration and beautiful AFM pictures of the magnetic filaments.

References

[1] Goubault C, Jop P, Fermigier M, Baudry J, Bertrand E and Bibette J 2003 *Phys. Rev. Lett.* **91** 260802
[2] Biswal S L and Gast A P 2003 *Phys. Rev.* E **68** 021402
[3] Cebers A 2005 *Curr. Opin. Colloid Interface Sci.* **10** 167
[4] Biswal S L and Gast A P 2004 *Anal. Chem.* **76** 6448
[5] Cebers A 2006 *J. Magn. Magn. Mater.* **300** 67
[6] Dreyfus R, Baudry J, Roper M L, Fermigier M, Stone H A and Bibette J 2005 *Nature* **437** 862
[7] Cebers A 2005 *Magnetohydrodynamics* **41** 63
[8] Cebers A 2003 *J. Phys.: Condens. Matter* **15** S1335
[9] Koenig A, Hebraud P, Gosse C, Dreyfus R, Baudry J, Bertrand E and Bibette J 2005 *Phys. Rev. Lett.* **95** 128301
[10] Lowe A E H *A Treatise on the Mathematical Theory of Elasticity* 4th edn (New York: Dover)
[11] Odijk T 1977 *J. Polym. Sci.* **15** 477
[12] Skolnick J and Fixman M 1977 *Macromolecules* **10** 944
[13] Roper M L, Dreyfus R, Baudry J, Fermigier M, Bibette J and Stone H A 2006 *J. Fluid Mech.* **554** 167